

Preventing carbon contamination of optical devices for X-rays: the effect of oxygen on photon-induced dissociation of CO on platinum

Paul Risterucci,^a Geog Held,^b Azzedine Bendounan,^{a*} Matthieu G. Silly,^a Christian Chauvet,^a Debora Pierucci,^a Nathan Beaulieu^a and Fausto Sirotti^a

^aSynchrotron SOLEIL, L'Orme des Merisiers, Saint-Aubin, BP 48, F-91192 Gif-sur-Yvette Cedex, France, and ^bDepartment of Chemistry, University of Reading, Whiteknights, Reading RG6 6AD, UK. E-mail: azzedine.bendounan@synchrotron-soleil.fr

Platinum is one of the most common coatings used to optimize mirror reflectivity in soft X-ray beamlines. Normal operation results in optics contamination by carbon-based molecules present in the residual vacuum of the beamlines. The reflectivity reduction induced by a carbon layer at the mirror surface is a major problem in synchrotron radiation sources. A time-dependent photoelectron spectroscopy study of the chemical reactions which take place at the Pt(111) surface under operating conditions is presented. It is shown that the carbon contamination layer growth can be stopped and reversed by low partial pressures of oxygen for optics operated in intense photon beams at liquid-nitrogen temperature. For mirrors operated at room temperature the carbon contamination observed for equivalent partial pressures of CO is reduced and the effects of oxygen are observed on a long time scale.

© 2012 International Union of Crystallography
Printed in Singapore – all rights reserved

Keywords: carbon contamination; beamline optics; surface chemistry; photoelectron spectroscopy.

1. Introduction

The interaction of carbon monoxide and oxygen on platinum surfaces is one of the most studied subjects in surface science. Owing to their structural simplicity these molecules can be studied by a variety of experimental and theoretical techniques and their reaction mechanisms are well understood. On the other hand their interaction is of fundamental importance to key technologies, such as purification of hydrogen for fuel cells (Steele & Heinzl, 2001) or catalytic conversion of car exhaust gases (Xie *et al.*, 2009). CO oxidation has been widely studied at low and ambient pressures (Ertl, 1994; Wintterlin *et al.*, 1997; Gao *et al.*, 2009; Hendriksen & Frenken, 2002). The present study investigates the X-ray-induced surface chemistry of CO and O₂ on the Pt(111) surface. It focuses on the kinetics of photon-induced dissociation of CO on Pt(111) and explores the possibility of removing the dissociation products by oxidation under the influence of soft X-rays. The experiments are strongly motivated by the desire to prevent carbon contamination of optical elements in soft X-ray and UV synchrotron beamlines, which are often coated with Pt in order to improve their reflectivity. Even with excellent base pressures in the 10⁻¹⁰ mbar range a significant increase in the partial pressures of carbon-containing molecules, mostly CO, is observed in the mirror chambers of such beamlines when the optical elements are irradiated. Continuous operation in CO partial pressures results in thick carbon layers on the

surfaces exposed to synchrotron radiation (Chauvet *et al.*, 2011). In the soft X-ray regime (<1 keV), where the monochromators operate with high deviation angles, carbon contamination leads to sharp absorption features in the photon intensity *versus* energy and has dramatic effects on the photon polarization. This makes accurate X-ray absorption spectroscopy near the carbon *K*-edge difficult at best, and often unreliable, and prevents spectroscopic studies of many carbon-based molecules. In order to enable a comparison with realistic beamline conditions, the experiments were carried out both with the sample at room temperature (RT) and cooled to liquid-nitrogen (LN) temperatures (around 85 K). The high power delivered by insertion devices at synchrotron radiation sources often makes it necessary to cool the first optical elements to cryogenic temperatures.

2. Experimental details

The measurements were performed taking advantage of the real-time chemical reactivity set-up available on the experimental station of the TEMPO beamline at the SOLEIL synchrotron radiation source (Polack *et al.*, 2010). The SCIENTA SES2002 electron energy analyzer and the beamline were operated at an overall resolution of about 25 meV at photon energy 380 eV and 50 meV for higher photon energy experiments (Bergeard *et al.*, 2011). The Pt(111) surface was

cleaned by cycles of Ar⁺ sputtering and annealing in oxygen pressure [30 min at 750 K with $P(\text{O}_2) = 1 \times 10^{-7}$ mbar] followed by flashing to 1200 K for 1 min. High-purity CO and O₂ were introduced in the experimental chamber during data acquisition; their partial pressures were monitored with a mass spectrometer. The photon flux density on the sample was maximized to reach 10^{16} photons s⁻¹ cm⁻², which is comparable with the photon flux density at beamline mirrors. With this photon density at the sample surface, the progress of CO adsorption and carbon contamination can be monitored by measuring the C-1s core-level binding energies (BE) in a photoelectron spectroscopy experiment.

3. Results and discussion

It is well established that CO molecules can occupy two different adsorption sites on Pt(111), atop and a twofold bridge site, in an upright geometry (Froitzheim *et al.*, 1977). They are clearly identified by the C-1s binding energies of 286.8 eV and 286.1 eV, respectively, as shown in the left-hand panel of Fig. 1, which is in excellent agreement with the literature (Kinne *et al.*, 2002; Bondino *et al.*, 2000). At the saturation coverage of 0.5 monolayer (ML) the surface is covered by equal amounts of atop and bridge-bonded molecules in a very stable $c(2 \times 4)$ overlayer structure (Kinne *et al.*, 2002; Bondino *et al.*, 2000). The spectra presented in Fig. 1 were measured at RT after 5 min and after 5 h of exposure to the soft X-ray beam. The measurements were performed with 380 eV photon energy under ultra-high-vacuum conditions after CO dosing for 10 min at 10^{-8} mbar to obtain the

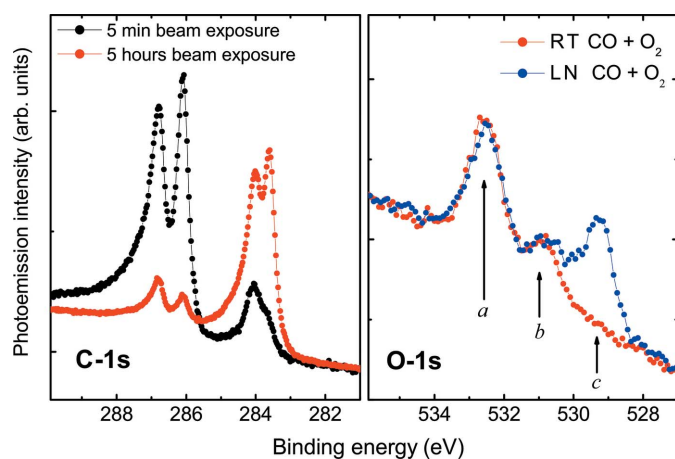


Figure 1

Left: carbon 1s photoemission spectra measured 5 min (black) and 5 h [grey (red online)] after CO dosing for 10 min in 10^{-8} mbar partial pressure at RT. The measurements were performed with 380 eV photon energy. The signatures of CO adsorption sites are located at BE 286.8 eV (atop) and 286.09 eV (bridge). The carbon contamination is characterized by two peaks at BE 284.0 eV and 283.6 eV. Right: oxygen 1s photoemission spectra measured with 630 eV photon energy at RT [grey (red online)] and at LN temperature [black (blue online)] after 10 min of simultaneous exposure at CO and O₂ partial pressure of 0.9×10^{-8} mbar and 4.9×10^{-8} mbar, respectively. Peaks indicated by *a* and *b* are assigned to the O-1s levels of the CO molecule on different sites on Pt(111), while peak *c* is associated with the O-1s of the oxygen.

formation of the saturation coverage. Already 5 min later a C-1s feature associated with dissociation can be detected in the BE region around 284 eV. Long exposure results in almost complete dissociation of the CO molecules. The two new peaks at BE 284.0 and 283.6 eV indicate the formation of a carbon layer with carbon atoms in two distinctly different chemical environments. These could be different adsorption sites on the Pt(111), *e.g.* hexagonal close-packed and face-centred cubic hollow sites or C–C bonded graphene-like *versus* isolated C atoms.

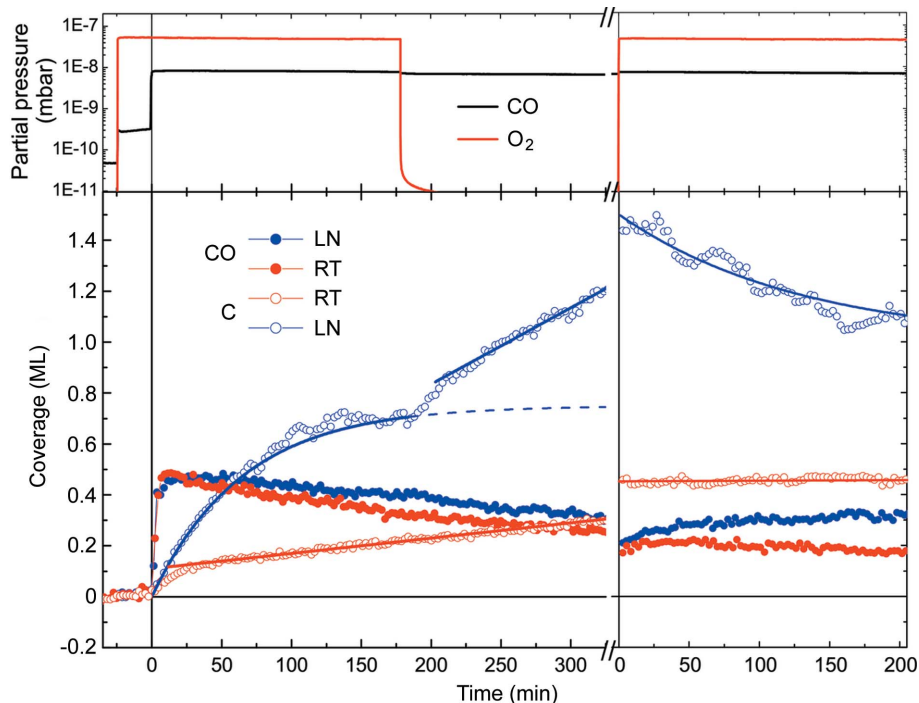
While the sticking probability of CO is almost independent of temperature between 85 K and RT, the adsorption of O₂ is strongly temperature dependent. Below 96 K, O₂ is known to be physisorbed, at higher temperatures the molecules dissociate and chemisorb (Gland *et al.*, 1980; Puglia *et al.*, 1995; Nolan *et al.*, 1999; Gustafsson & Andersson, 2004; Stipe *et al.*, 1997). The physisorbed species is characterized by an O-1s BE of 535.0 eV whereas the chemisorbed atoms lead to a signal at BE 529.7 eV (Kim *et al.*, 2010). Kim and co-workers showed that synchrotron radiation can dissociate O₂ molecules at cryogenic temperatures (Kim *et al.*, 2010).

As found by several previous studies, CO oxidation does not take place on Pt(111) below 120 K (Kinne *et al.*, 2004; Allers *et al.*, 1994), but when CO and O are co-adsorbed at higher temperatures the reaction probability is almost 1, following a Langmuir–Hinshelwood mechanism (Allers *et al.*, 1994; Campbell *et al.*, 1980). The rate-limiting process at low temperature is the dissociation of O₂. When irradiated with an intense soft X-ray beam, however, this dissociation can be photon-induced and the oxidation reactions $\text{C} + \text{O} \rightarrow \text{CO}$ and $\text{CO} + \text{O} \rightarrow \text{CO}_2$ can proceed.

The kinetics of photon-induced surface processes were monitored by measuring both C-1s and O-1s core-level spectra with a photon energy of 630 eV. This way, the chemical species (peak binding energy) as well as their coverages (peak area) can be recorded in real time during the experiment. In Fig. 2 we present the evolution of the signals related to CO and atomic carbon at RT and LN temperature over a period of 7 h. The data points represent the integrated photoemission intensity after background subtraction for the BE regions 287.2 to 285.7 eV (CO, filled circles) and 284.3 to 283.3 eV (atomic carbon, open circles). The intensity axis is re-scaled such that the signal of the saturated layer at RT corresponds to 0.5 ML. The CO and O₂ partial pressures are plotted at the top of Fig. 2.

At the beginning of the experiment, oxygen is introduced into the chamber at a pressure $P(\text{O}_2) = 4.9 \times 10^{-8}$ mbar. At $t = 0$ s, 0.9×10^{-8} mbar CO is added to the gas mixture and the evolution of the C-1s signal is recorded over a period of 3 h. On the time scale of Fig. 2 the surface is saturated by CO almost immediately at both temperatures. Under irradiation by the photon beam, the amount of intact CO on the surface then decreases at a longer time scale while the signal associated with contaminating carbon atoms increases.

The growth of the carbon layer is much faster at LN temperatures [black symbols (blue online)] than at RT [grey symbols (red online)]. The former can be described by $\Theta_{\text{C}} =$


Figure 2

Left-hand panel: the lower part represents the time evolution of the CO (filled symbols) and C (open symbols) XPS peak intensities (with photon energy 630 eV). The measured peak areas were normalized such that the CO saturation coverage at RT corresponds to 0.5 ML. The figure shows corresponding experiments at RT [grey symbols (red online)] and at LN temperature [black symbols (blue online)]. The upper part shows mass spectrometer measurements of the partial pressures at LN temperature. A CO partial pressure of 0.9×10^{-8} mbar is introduced into the chamber at $t = 0$ s. 15 min after, O₂ partial pressure of 4.9×10^{-8} mbar has been introduced. In both experiments the surface is exposed to CO and O₂ with a partial pressure ratio $P(\text{O}_2)/P(\text{CO}) = 5$. After 285 min the O₂ partial pressure is switched off. Right-hand panel: contaminated surfaces resulting from the previous experiment are exposed again to a mixture of CO and O₂ with a partial pressure ratio $P(\text{O}_2)/P(\text{CO}) = 5$.

$\Theta_{\max}[1 - \exp(-t/\tau)]$ with a characteristic time, τ , of 65 min and a saturation coverage, Θ_{\max} , of 0.75 ML. The O-1s spectra measured at low temperature (not shown here) indicate that around 1 ML of physisorbed O₂ molecules is present on the surface. Under the above conditions [$P(\text{O}_2) = 4.9 \times 10^{-8}$ mbar, $P(\text{CO}) = 0.9 \times 10^{-8}$ mbar, $T \approx 85$ K] we observe that the carbon layer growth stops when a maximum coverage of 0.75 ML is reached. When the oxygen dosing is stopped (at $t = 160$ min in Fig. 2) at low temperature the contamination signal starts to grow again, at a constant rate of 0.18 ML h^{-1} , which does not seem to be affected even at the point where the Pt(111) surface is covered by a full monolayer of carbon atoms. This and the fact that a significant CO signal with the same BEs is still observed at this point indicates cluster-like three-dimensional growth of the carbon contamination. On the right-hand side of Fig. 2 we present the behavior observed if O₂ is re-introduced into the chamber after a thick carbon layer has been grown. At low temperature this reduces the carbon contamination signal significantly with a characteristic time of 130 min, compatible with reaching a sub-monolayer coverage similar to the saturation coverage of ~ 0.75 ML found in the first part of the experiment. In Fig. 2 one can observe that the thickness of the carbon contamination is lower than that measured with lower photon energy without

permanent CO dosing (presented in Fig. 1). The relative contributions of the photon flux, photon energy and gas pressure on the carbon contamination process goes beyond the aim of the present work and must be studied in more detail.

Although the signal of intact CO decreases at a similar rate for both temperatures, the increase in the contamination signal is slower at room temperature. After a steeper increase in the first 25 min, the carbon coverage increases at a constant rate of 0.036 ML h^{-1} and reaches a stable saturation coverage of 0.45 ML in the presence of oxygen (right-hand panel).

There is no change in the growth rate when oxygen is removed from the chamber; the build-up of the carbon layer at room temperature is not affected by the presence of O₂. Since the carbon contamination process is slower at room temperature, the effect of the oxygen exposure requires much longer experimental sessions to obtain a better description of the phenomenon taking place on the real optical elements of the beamline.

The faster build-up of atomic carbon at low temperatures is most likely related to the fact that the oxidative removal of atomic carbon, $\text{C} + \text{O} \rightarrow$

CO, is thermally activated. The rate-limiting step is O₂ dissociation. Therefore, if atomic oxygen can be supplied by photodissociation of O₂ the reaction can still proceed even at low temperature. The confirmation comes from the comparison of the O-1s core levels measured at low temperature and at room temperature after 10 min of O₂ and CO exposure (see right-hand panel of Fig. 1). At this stage of the reaction CO molecules are still present on the surface as indicated by the *a* and *b* O-1s peaks at 532.5 and 531 eV but at cryogenic temperature activated oxygen is also observed on the surface (peak at 529.3 eV binding energy). O-1s spectra measured as a function of time show that a constant amount of O₂ does adsorb on the surface also when atomic carbon is present. Note that the presence of this oxygen amount on the optical surface induces a reduction of photon flux at the oxygen *K*-edge of about 10%. The rate of oxidative removal of carbon increases with the amount of carbon on the surface until an equilibrium is reached. The same mechanism also explains the removal of the thick carbon layer after the oxygen supply had been interrupted (Fig. 2). From the kinetic constants determined in our experiment we estimate the photodissociation cross section for CO as 10^{-19} cm^2 ; the photon-induced oxidation has a rate of around $10^{-4} \text{ ML s}^{-1}$. At RT thermally activated oxygen is not available on the surface. The oxidation

of carbon runs in parallel with CO oxidation, $\text{CO} + \text{O} \rightarrow \text{CO}_2$, and balances the photon-induced dissociation of CO.

4. Conclusion

In summary, we have reproduced the carbon contamination conditions of Pt-coated mirrors in a surface science experiment. We have identified the binding energies of the carbon contaminating species and followed in real time the chemical reactions taking place at the Pt surface at RT and at LN temperature. For mirrors kept at LN temperature the presence of a relatively low O_2 partial pressure in the 10^{-8} mbar range in the chamber prevents the carbon contamination growth and reduces a thick carbon layer in the submonolayer range. Our findings are confirmed by the operation of the TEMPO beamline under real conditions, where the same partial pressures described above are now applied in our mirror chambers hosting LN-cooled mirrors. In the last year of operation we have not observed significant carbon contamination in contrast to the experience before when no oxygen was introduced. For mirrors operated at RT and in the presence of oxygen partial pressure, the carbon contamination layer appears to be saturated at only 0.45 ML. Such an observation needs to be further explored with much longer experimental sessions.

References

- Allers, K. H., Pfnür, H., Feulner, P. & Menzel, D. (1994). *J. Chem. Phys.* **100**, 3985–3998.
- Bergeard, N., Silly, M. G., Krizmancic, D., Chauvet, C., Guzzo, M., Ricaud, J. P., Izquierdo, M., Stebel, L., Pittana, P., Sergio, R., Cautero, G., Dufour, G., Rochet, F. & Sirotti, F. (2011). *J. Synchrotron Rad.* **18**, 245–250.
- Bondino, F., Comelli, G., Esch, F., Locatelli, A., Baraldi, A., Lizzit, S., Paolucci, G. & Rosei, R. (2000). *Surf. Sci.* **459**, L467–L474.
- Campbell, C. T., Ertl, G., Kuipers, H. & Segner, J. (1980). *J. Chem. Phys.* **73**, 5862–5873.
- Chauvet, C., Polack, F., Silly, M. G., Lagarde, B., Thomasset, M., Kubsy, S., Duval, J. P., Risterucci, P., Pilette, B., Yao, I., Bergeard, N. & Sirotti, F. (2011). *J. Synchrotron Rad.* **18**, 761–764.
- Ertl, G. (1994). *Surf. Sci.* **299–300**, 742–754.
- Froitzheim, H., Hopster, H., Ibach, H. & Lehwald, S. (1977). *Appl. Phys.* **13**, 147–151.
- Gao, F., Wang, Y., Cai, Y. & Goodman, D. W. (2009). *J. Phys. Chem. C*, **113**, 174–181.
- Gland, J. L., Sexton, B. A. & Fisher, G. B. (1980). *Surf. Sci.* **95**, 587–602.
- Gustafsson, K. & Andersson, S. (2004). *J. Chem. Phys.* **120**, 7750–7754.
- Hendriksen, B. L. M. & Frenken, J. W. M. (2002). *Phys. Rev. Lett.* **89**, 046101.
- Kim, Y. S., Bostwick, A., Rotenberg, E., Ross, P. N., Hong, S. C. & Mun, B. S. (2010). *J. Chem. Phys.* **133**, 034501.
- Kinne, M., Fuhmann, T., Whelan, C. M., Zhu, J. F., Pantförder, J., Probst, M., Held, G., Denecke, R. & Steinrück, H. P. (2002). *J. Chem. Phys.* **117**, 10852–10859.
- Kinne, M., Fuhrmann, T., Zhu, J. F., Whelan, C. M., Denecke, R. & Steinrück, H. P. (2004). *J. Chem. Phys.* **120**, 7113–7122.
- Nolan, P. D., Lutz, B. R., Tanaka, P. L., Davis, J. E. & Mullins, C. B. (1999). *J. Chem. Phys.* **111**, 3696–3704.
- Polack, F., Silly, M. G., Chauvet, C., Lagarde, B., Bergeard, N., Izquierdo, M., Chubar, O., Krizmancic, D., Ribbens, M., Duval, J. P., Basset, C., Kubsy, S. & Sirotti, F. (2010). *AIP Conf. Proc.* **1234**, 185–188.
- Puglia, C., Nilsson, A., Hernnäs, B., Karis, O., Bennich, P. & Martensson, N. (1995). *Surf. Sci.* **342**, 119–133.
- Steele, B. C. H. & Heinzl, A. (2001). *Nature (London)*, **414**, 345–352.
- Stipe, B. C., Rezaei, M. A. & Ho, W. (1997). *J. Chem. Phys.* **107**, 6443–6447.
- Wintterlin, J., Völkening, S., Janssens, T. V. W., Zambelli, T. & Ertl, G. (1997). *Science*, **278**, 1931–1934.
- Xie, X., Li, Y., Liu, Z.-Q., Haruta, M. & Shen, W. (2009). *Nature (London)*, **458**, 746–749.